LETTER

doi:10.1038/nature11561

Dark material on Vesta from the infall of carbonaceous volatile-rich material

T. B. McCord[1], J.-Y. Li[2], J.-P. Combe[1], H. Y. McSween[3], R. Jaumann[4], V. Reddy[5,6], F. Tosi[7], D. A. Williams[8], D. T. Blewett[9], D. Turrini[7], E. Palomba[7], C. M. Pieters[10], M. C. De Sanctis[7], E. Ammannito[7], M. T. Capria[7], L. Le Corre[5], A. Longobardo[7], A. Nathues[5], D. W. Mittlefehldt[11], S. E. Schröder[5], H. Hiesinger[12], A. W. Beck[13], F. Capaccioni[7], U. Carsenty[4], H. U. Keller[14], B. W. Denevi[9], J. M. Sunshine[15], C. A. Raymond[16] & C. T. Russell[17]

Localized dark and bright materials, often with extremely different albedos, were recently found on Vesta's surface[1,2]. The range of albedos is among the largest observed on Solar System rocky bodies. These dark materials, often associated with craters, appear in ejecta and crater walls, and their pyroxene absorption strengths are correlated with material brightness. It was tentatively suggested that the dark material on Vesta could be either exogenic, from carbon-rich, low-velocity impactors, or endogenic, from freshly exposed mafic material or impact melt, created or exposed by impacts. Here we report Vesta spectra and images and use them to derive and interpret the properties of the 'pure' dark and bright materials. We argue that the dark material is mainly from infall of hydrated carbonaceous material (like that found in a major class of meteorites and some comet surfaces[3–5]), whereas the bright material is the uncontaminated indigenous Vesta basaltic soil. Dark material from low-albedo impactors is diffused over time through the Vestan regolith by impact mixing, creating broader, diffuse darker regions and finally Vesta's background surface material. This is consistent with howardite–eucrite–diogenite meteorites coming from Vesta.

Vesta has a mean diameter[6] of 525 km and is the second-most massive object in the main asteroid belt of our Solar System, smaller than Ceres and similar to Pallas. These three bodies form a separate class of intact objects in the asteroid belt that have experienced planetary processes[7], such as thermal evolution[8] powered by short-lived radionuclides incorporated at the time of accretion. This process in general results in mineralogical alteration due to heating, and differentiation, with denser materials sinking towards the centre. In contrast, most other main-belt asteroids seem to be pieces of collisionally disrupted objects. Although subdued albedo differences on global[9] and broadly regional[10] scales were known to exist from telescopic observations, localized and intense dark and bright occurrences were not anticipated (see Supplementary Information).

We used photometrically uniform near-global albedo spectral image mosaics constructed from the Dawn[11] Framing Camera and

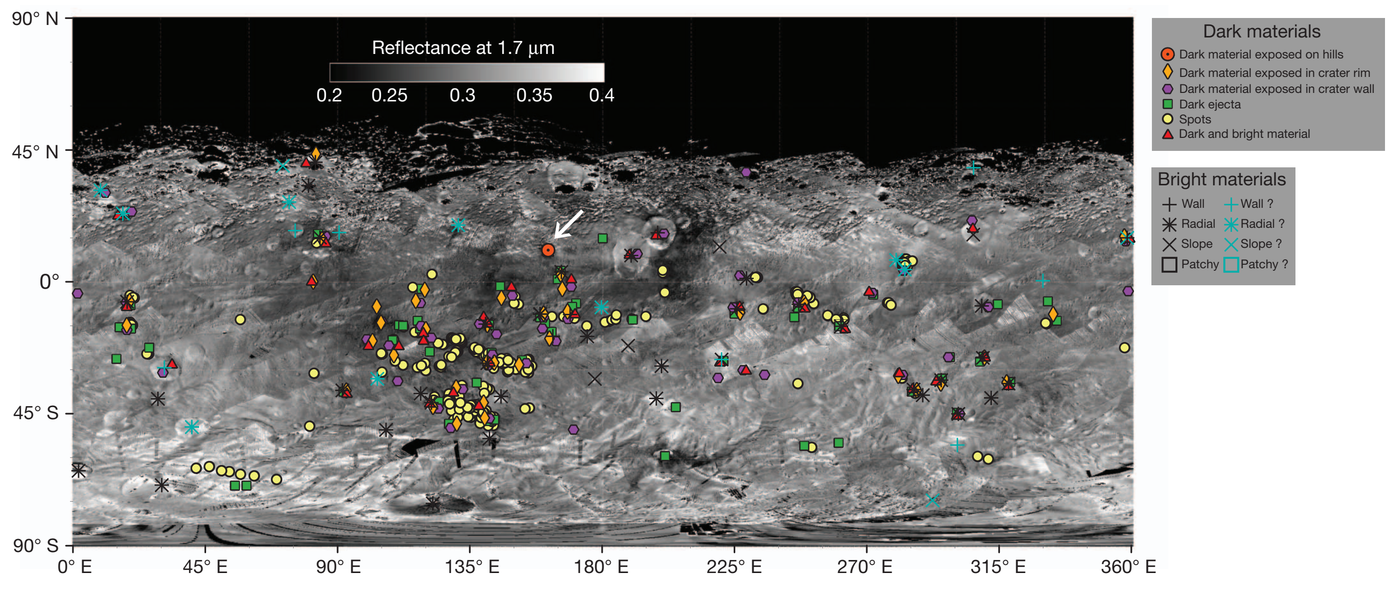

Figure 1 | Locations of dark and bright material. Mapped occurrences of local dark- and bright-material locations (points) are shown here plotted on a 1.7-µm albedo map derived from VIR images. The albedo mosaic also exhibits broad low-albedo regions, especially between about 70° and 220° longitude, near which the localized dark-material points tend to cluster, suggesting a causal relationship. Bright- and dark-material local examples tend not to be uniformly distributed or correlated with each other. For this base map, the entire VIR infrared data set from late Approach, Survey and High-Altitude Mapping orbits was converted into reflectance and mosaicked.

[1]Bear Fight Institute, 22 Fiddler's Road, Box 667, Winthrop, Washington 98862, USA. [2]Planetary Science Institute, Tucson, Arizona 85719, USA. [3]University of Tennessee, Knoxville, Tennessee 37996, USA. [4]DLR, Institute of Planetary Research, Berlin, 80302, Germany. [5]Max Planck Institute for Solar System Research, Max-Planck-Strasse 2, 37191 Katlenburg, Germany. [6]University of North Dakota, Grand Forks, North Dakota 58202, USA. [7]Istituto Nazionale di Astrofisica (IASF), Via Fosso del Cavaliere 100, Rome 00133, Italy. [8]ASU, Tempe, Arizona 85287, USA. [9]Johns Hopkins University Applied Physics Laboratory, Laurel, Maryland 20723, USA. [10]Brown University, Providence, Rhode Island 02912, USA. [11]Astromaterials Research Office, NASA Johnson Space Center, Houston, Texas 77058, USA. [12]Institut für Planetologie, Westfälische Wilhelms-Universität Münster, Schlossplatz 2, 48149 Munster, Germany. [13]Department of Mineral Sciences, Smithsonian National Museum of Natural History, Washington DC 20024, USA. [14]Institut für Geophysik und extraterrestrische Physik, Mendelssohnstrasse 3, 38106 Braunschweig, Germany. [15]Department of Astronomy, University of Maryland, College Park, Maryland 20742, USA. [16]California Institute of Technology, Jet Propulsion Laboratory, Pasadena, California 91109, USA. [17]University of California, Los Angeles, California 90095, USA.

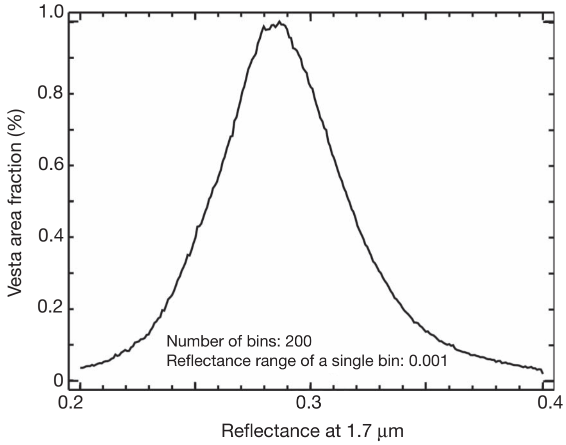

Figure 2 | Frequency distribution of albedos. The global distribution of albedos at 1.7 µm, derived from the infrared global base map (Fig. 1) at a spatial resolution of about 1 km. The curve represents surface area fraction (not number of pixels). At higher resolutions this distribution would develop smaller peaks at each extreme of brightness, representing individual dark- and bright-material locations. At this resolution, the broad global distribution represents mixing between dark and bright materials.

the visible and infrared mapping spectrometer (VIR) to demonstrate that dark and bright materials are distributed non-uniformly and are uncorrelated (as seen in Fig. 1), suggesting different origins. Unlike bright material, some dark material also occurs over larger areas with more diffuse boundaries.

Investigation of the 1.7-µm albedo frequency distribution at the spatial scale of 1 km per pixel surprisingly showed it to be unimodal, lacking any special albedo classes (Fig. 2). The bright material appears to be distinct from dark material on a local scale[1,2], but globally at this resolution these albedo classes form a continuum distribution with a peak at the global average albedo. This suggests a mixing of dark and bright materials to produce the range of Vesta surface materials.

We compared VIR infrared spectra for dark and bright material (Fig. 3). The pyroxene signature clearly dominates Vesta's spectra globally[8] and in detail[2,12], a product of Vesta's igneous past[8]. Dark material has weaker apparent absorptions[2]. We then applied a Multiple-Endmember Linear Spectral Unmixing Model[13] to derive the spectrum of each of Vesta's surface materials within each VIR pixel, using the fewest possible spectral endmembers. We found that the VIR spectra could be modelled using the weighted sum of only two spectral endmembers, called 'bright' and 'dark' materials in Fig. 3. The modelled dark-material endmember spectrum shows no absorption bands, with a reddish slope that flattens towards longer wavelengths. The modelled bright-material endmember spectrum shows the classic, strong pyroxene 2-µm band and the expected pyroxene continuum shape[8,12]. Our conclusion is that, for the most part, Vesta's surface material can be thought of as having two spectral components—the dark and bright endmember spectra—in different proportions. This is consistent with the mixing-process hypothesis and suggests that the dark spectral component is the agent diluting the pyroxene spectral signature. The identity of the bright endmember is probably the intrinsic Vesta basaltic soil, rich in unaltered, crystalline pyroxenes. This relationship between bright and dark materials is further supported by the strong correlation of the 1-µm pyroxene absorption band strength with albedo from analysis of the Framing Camera colour data[2] and shown here (Fig. 4). We note that the dark-material spectrum is very similar to that of carbonaceous chondrite material, such as is found in a major class of meteorites (the carbonaceous chondrites).

Regions of Vesta where the residuals from the spectral mixing analysis are largest (but still small) have some of the strongest pyroxene signatures. These represent the best opportunity to study intrinsic Vesta material, for example, at some apparent impact structures that may be sampling ejecta from the Rheasilvia basin near the south pole.

Suggestions for the origin of discrete areas of dark material include indigenous sources (such as opaque-rich lava flows and impact melts) as well as contamination from exogenous material (delivered from foreign, impacting bodies). A search of Dawn VIR spectra for OH spectral features near 3 µm was made[14,15], prompted by the discovery of OH and H_2O in the lunar surface. A 2.8-µm absorption was found[16] and its analysis indicates[17] that the dark material appears to be relatively enriched in OH (Fig. 5). Carbonaceous chondrite meteorite material often contains 10–20% OH-bearing hydrated minerals, whereas none of the other suggested dark-material sources contain

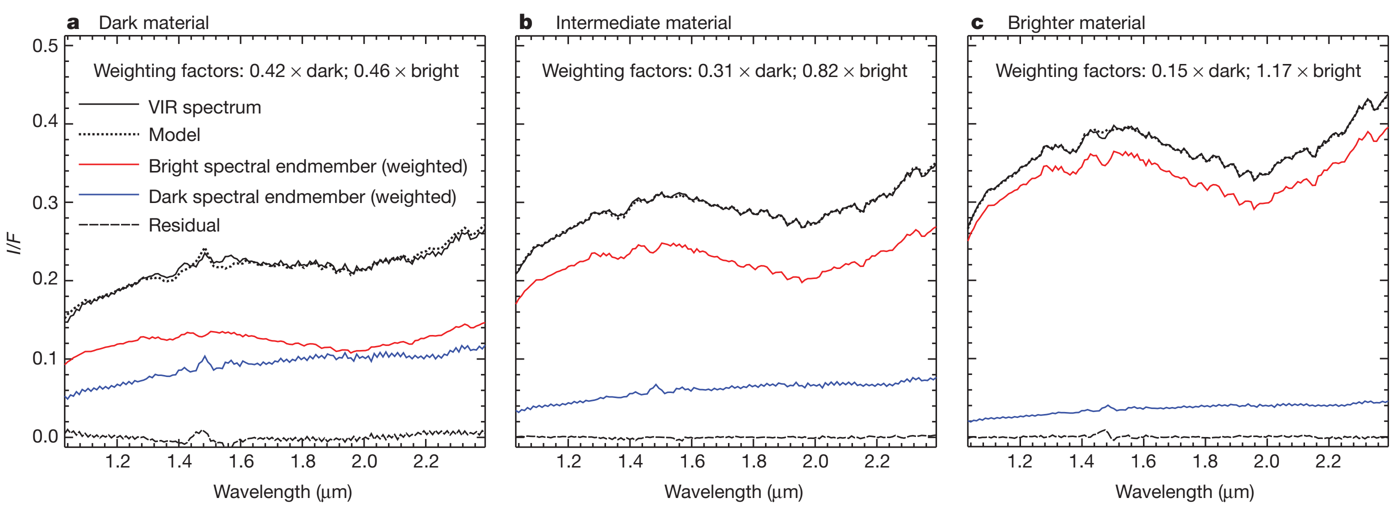

Figure 3 | Reflectance spectra of dark and bright materials. $I/F = \pi R/(d^2F)$, where R is the spectral radiance of the target's surface in units of $W\,m^{-2}\,sr^{-1}\,\mu m^{-1}$, F is the spectral irradiance or solar flux in units of $W\,m^{-2}\,\mu m^{-1}$ and d is the distance between the Sun and the target. Reflectance spectra for a representative VIR scene (366894613) illustrate Vesta spectra modelling results for three different types of units near the region indicated by the white arrow in Fig. 1. **a**, The VIR dark-material unit spectrum (solid black line) is modelled using the two weighted endmember spectra (red and blue spectra). The model result is the dotted black line overlying the VIR spectrum; the resulting residual is shown as a dashed black line. The residual shows no distinctive features and overall is near the noise level of the VIR data, suggesting successful modelling. (The feature near 1.44 µm is a calibration artefact.) **b**, **c**, Similar examples for intermediate and brighter materials nearby. The weighting factors are given on the plots and the mixture spectrum is calculated as the weighted sum of dark + bright. This analysis was performed at several other areas with similar results, before we successfully modelled the entire mosaic shown in Fig. 1.

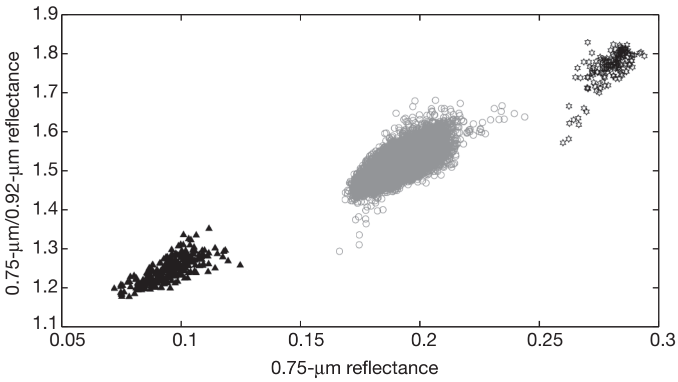

Figure 4 | Correlation of pyroxene absorption with material reflectance. The strength of the '1-µm' pyroxene absorption, measured by the ratio of reflectance at 0.75 µm to that at 0.92 µm, is strongly correlated with the reflectance in the continuum (0.75 µm), shown here for three example regions. Data are from the framing camera[2]. Greater ratio values correspond to stronger absorption bands. Dark (black filled circles) and bright (black open circles) areas cluster near the extremes of the plot, while background material (grey open circles) appears near the middle of this apparent mixing line. Dark material pixels are from Cornelia crater (9.3° S, 225.5° E), background material is from an area located between 5° S–17° N, 320° E–356° E and the bright material is from Tuccia crater (40° S, 197° E) in the Claudia coordinate system used by Dawn. If the entire surface of Vesta were treated here, rather than only example areas, the three clusters of points would merge into a continuum from least to greatest reflectance.

OH. Further, the Gamma Ray and Neutron Detector investigation reports[18] excess H (without identifying the molecular form) for certain regions that correspond with the broader darker areas shown in Fig. 1.

The most common group of differentiated meteorites, the howardite–eucrite–diogenites (HEDs), display reflectance spectra strongly suggesting that they originated from Vesta[8]. Three types of dark materials occur in the HEDs[19]: clasts of carbonaceous chondrite material in howardites, impact melts and shock-blackened materials in HED breccias, and fine-grained eucrites with quenched textures. These dark components occur in a few samples up to 60 per cent by volume but more typically compose a few per cent by volume of the rocks[20,21]. Although several types of dark material exist in the HEDs, only the

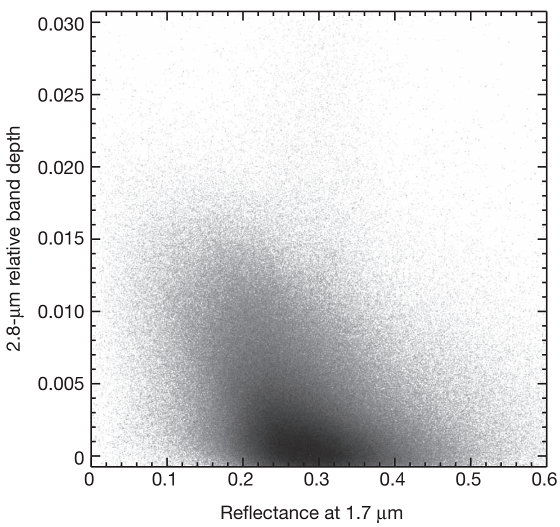

Figure 5 | Correlation of OH spectral absorption with material reflectance. Two-dimensional scatter plot from global observations of Vesta by VIR show a diffuse anti-correlation of the OH-related 2.8-µm-absorption band depth[9,15] and Vesta's reflectance at 1.7 µm (Fig. 1). The OH signature is correlated with the dark material in Vesta's surface.

carbonaceous material is consistent with the properties of the dark constituent of Vesta's surface.

It is plausible that enough dark material to match what we observe could be delivered on Vesta by low albedo (probably carbonaceous) asteroids over time. In addition to Vesta's small size and surface gravity, its location in the asteroid belt implies that most impacts occur at lower velocities, favouring the preservation of a larger fraction of the impacting material (see Supplementary Information). Analytical estimates we performed (see Supplementary Information) indicate that about 300 low-albedo asteroids with diameters between 1 km and 10 km could have impacted Vesta during the last 3.5 billion years, that is, once the asteroid belt assumed its present structure[22]. These impactors would deliver to the Vestan surface about $(3–4) \times 10^{18}$ g of low-albedo, probably carbonaceous material. This mass would be enough to wrap Vesta in a thick dark blanket 1–2 m thick. Impact gardening would occur, creating a dark crustal mixed zone to a depth of one to several kilometres. Further, it is well documented that the addition of small amounts of fine-grained opaque material to a semi-transparent material (such as Vesta's pyroxene-rich surface) reduces the reflectance of the mixture in a highly effective, nonlinear manner[23].

Thus, we see on Vesta a dramatic example of a common process that must affect many Solar System objects: that of contamination and alteration of indigenous surfaces owing to impact and retention and mixing of the impactor material. This process also provides a mechanism by which to transport hydrated and organic-rich materials to Vesta and other bodies. This hypothesis is consistent with evidence observed in the HED meteorites[19] and strengthens the connection between the HEDs and Vesta[8,19].

Received 16 June; accepted 29 August 2012.

1. Jaumann, R. *et al.* Vesta's shape and morphology. *Science* **336,** 687–690 (2012).
2. Reddy, V. *et al.* Color and albedo heterogeneity of Vesta from Dawn. *Science* **336,** 700–704 (2012).
3. Sandford, S. A. *et al.* Organics captured from comet 81P/Wild 2 by the Stardust Spacecraft. *Science* **314,** 1720–1724 (2006).
4. Sunshine, J. M. *et al.* Exposed water ice deposits on the surface of comet 9P/Temple 1. *Science* **311,** 1453–1455 (2006).
5. Gibb, E. L. *et al.* The organic composition of C/2001 A2 (LINEAR). II. Search for heterogeneity within a comet nucleus. *Icarus* **188,** 224–232 (2007).
6. Russell, C. T. *et al.* Dawn at Vesta: testing the protoplanetary paradigm. *Science* **336,** 684–686 (2012).
7. McCord, T. B., McFadden, L. A., Russell, C. T., Sotin, C. & Thomas, P. C. Ceres, Vesta, and Pallas: protoplanets, not asteroids. *Trans. AGU* **87,** 105–109 (2006).
8. McCord, T. B., Adams, J. B. & Johnson, T. V. Asteroid Vesta: spectral reflectivity and compositional implications. *Science* **168,** 1445–1447 (1970).
9. Degewij, J., Tedesco, E. F. & Zellner, B. H. Albedo and color contrasts on asteroid surfaces. *Icarus* **40,** 364–374 (1979).
10. Zellner, B. H. *et al.* Hubble Space Telescope images of asteroid 4 Vesta in 1994. *Icarus* **128,** 83–87 (1997).
11. Russell, C. T. & Raymond, C. A. The Dawn mission to Vesta and Ceres. *Space Sci. Rev.* **163,** 3–23 (2011).
12. De Sanctis, M. C. *et al.* Spectroscopic characterization of mineralogy and its diversity across Vesta. *Science* **336,** 697–700 (2012).
13. Combe, J.-Ph. *et al.* Analysis of OMEGA/Mars Express data hyperspectral data using a Multiple-Endmember Linear Spectral Unmixing Model (MELSUM): methodology and first results. *Planet. Space Sci.* **56,** 951–975 (2008).
14. Combe, J.-Ph. *et al.* Water and other volatiles on Vesta after the lunar case. *Lunar Planet. Sci. Conf.* **431,** 2463 (2012).
15. De Sanctis, M. C. *et al.* Detection of widespread hydrated materials on Vesta by VIR imaging spectrometer on board the Dawn mission. *Astrophys. J. Lett.* **758,** L36 (2012).
16. Pieters, C. M. *et al.* Character and spatial distribution of OH/H_2O on the surface of the Moon seen by M^3 on Chandrayaan-1. *Science* **326,** 568–572 (2009).
17. McCord, T. B. *et al.* Sources and physical processes responsible for OH/H_2O in the lunar soil as revealed by the Moon Mineralogy Mapper (M^3), *J. Geophys. Res.* **116,** E00G05 (2011).
18. Prettyman, T. H. *et al.* Elemental mapping by Dawn reveals exogenic H in Vesta's regolith. *Science* doi:10.1126/science.1225354.
19. McSween, H. Y., Mittlefehldt, D. W., Beck, A. W., Mayne, R. G. & McCoy, T. J. HED meteorites and their relationship to the geology of Vesta and the Dawn mission. *Space Sci. Rev.* **163,** 141–174 (2011).
20. Zolensky, M. E., Weisberg, M. K., Buchanan, P. C. & Mittlefehldt, D. W. Mineralogy of carbonaceous chondrite clasts in HED achondrites and the Moon. *Meteorit. Planet. Sci.* **31,** 518–537 (1996).
21. Beck, A. W., Welten, K. C., McSween, H. Y., Viviano, C. E. & Caffee, M. W. Petrologic and textural diversity among the PCA 02 howardite group, one of the largest pieces of the Vestan surface. *Meteorit. Planet. Sci.* **47,** 947–969 (2012).

22. Coradini, A., Turrini, D., Federico, C. & Magni, G. Vesta and Ceres: crossing the history of the Solar System. *Space Sci. Rev.* **163,** 25–40 (2011).
23. Clark, R. N. Spectral properties of mixtures of montmorillonite and dark grains—implications for remote sensing minerals containing chemically and physically adsorbed water. *J. Geophys. Res.* **88,** 10635–10641 (1983).

Supplementary Information is available in the online version of the paper.

Acknowledgements This research was supported by the NASA Dawn Project under contract from UCLA, by the NASA Dawn at Vesta Participating Scientist program, the Italian Space Agency, the Max Planck Institute for Solar System Research, and the Germany Aerospace Agency (DLR). We acknowledge the support of the Dawn Science, Instrument and Operations Teams.

Author Contributions T.B.McC. designed the study, directed the research and wrote the manuscript; J.-P.C., J-Y.L. and H.Y.McS. were the major contributors helping to design the study, direct the research and write the manuscript. D.T., T.B.McC. and J.-P.C. wrote the Supplementary Information. J.-P.C. performed the spectral unmixing of the VIR mapping spectrometer data and the correlation of OH with albedo. J.-P.C. and F.T. produced global maps from the VIR mapping spectrometer data. V.R. performed the correlation of albedo with band strength. L.L.C. and R.J. produced global mapping of Vesta with Framing Camera images. H.Y.McS., V.R. and D.W.M. contributed to the laboratory analysis of Vestan meteorites. J.-P.C., E.P., E.A., M.C.D.S. and A.L. contributed to the location of dark materials and to the spectral analysis of hydroxyl-rich areas from the VIR mapping spectrometer data. R.J. provided the location of dark materials from Framing Camera images. D.T. provided estimates of amounts of dark material coming from carbonaceous chondrite meteorites. J.-P.C., J-Y.L., F.C., E.P. and A.L. contributed to the photometric correction for the VIR mapping spectrometer. J-Y.L., S.E.S. and L.L.C. contributed to the photometric correction of Framing Camera images. F.T. and J.-P.C. investigated the need for thermal emission correction of the VIR mapping spectrometer. D.A.W. contributed much of the geologic context of dark material, developed example site descriptions, and wrote or edited geological context materials. D.T.B. participated in developing the dark-material interpretation and edited the manuscript. C.M.P. participated in providing context for the mixing effects on the resulting surface material and integrating space-weathering concepts. M.C.D.S. is the Principal Investigator of the VIR mapping spectrometer and helped to provide the VIR data. A.N. is the Principal Investigator of the Framing Camera and helped to provide the Framing Camera data. M.T.C. and F.C. analysed the thermal properties of the surface of Vesta. D.W.M. located bright materials from Framing Camera images. E.A., F.C., F.T., A.L., M.C.D.S. and J.-P.C. contributed to the calibration of the VIR mapping spectrometer. A.N., S.E.S. and V.R. contributed to the calibration of the Framing Camera. E.A. contributed to the sequencing of data acquisition for the VIR mapping spectrometer. S.E.S. contributed to the sequencing of data acquisition for the Framing Camera. H.H. contributed to the design and development of the Framing Camera. A.W.B., U.C., H.U.K., B.W.D. & J.M.S. participated in the working group studying the bright material. C.A.R. is the deputy Principal Investigator of the Dawn mission. C.T.R. is the Principal Investigator of the Dawn mission. All authors discussed the results and commented on the manuscript.

Author Information Data from the Dawn mission are publicly available through the NASA Planetary Data System. Reprints and permissions information is available at www.nature.com/reprints. The authors declare no competing financial interests. Readers are welcome to comment on the online version of the paper. Correspondence and requests for materials should be addressed to T.B.M. (tmccord@bearfightinstitute.com) or J.-P.C. (jean-philippe_combe@bearfightinstitutute.com).